

Monitoring of Rail/Wheel Interaction using Acoustic Emission

Nirav Ashokkumar Thakkar

Submitted for the degree of doctor of philosophy on completion of research in the School of Engineering and Physical Sciences, Mechanical Engineering, Heriot-Watt University

June 2009

This copy of the thesis has been supplied on condition that anyone who consults it is understood to recognise that the copyright rests with its author and that no quotation from the thesis and no information derived from it may be published without the prior written consent of the author or of the University (as may be appropriate)

Abstract

The work presented in this thesis is related to the condition monitoring of rail-wheel interaction using Acoustic Emission (AE), the principle being that both normal and abnormal rolling give rise to AE, features of which are related to the mechanical intensity of the interaction and hence the stress range (or stress intensity factor range) to which sections of track is being exposed.

Most of the work was carried out on a model wheel running on a model circular track, which was first characterised using a simulated source before studying the wave propagation from a continuously moving (wheel) source. Using a number of sensor arrays placed on the track, primary wave propagation characteristics such as wave speeds and attenuation coefficients and also secondary wave propagation characteristics such as reflection and transmission from and through the joint. A high speed camera was used to confirm, that wheel slip does not occur at the wheel speeds and loads of interest. A simple analytical model was derived using the measured wave propagation characteristics which describes the expected AE recorded at a track-mounted sensor as the wheel approaches and recedes.

Using the analytical model, the effect of increasing wheel speed and axle load on the normal rolling signal was measured. Wheel rattling was observed, particularly at lower wheel speeds and loads, and this was eliminated in some trails by introducing a spacer. The effect of minor track defects and wheel flange rubbing on the track was also studied, where the comparison of the expected normal running signal with excursions above background allowed the locations of track defects to be identified. Finally, a set of experiments were carried out with simulated wheel defects. The signals were analysed using the principle of demodulated frequency resonance and matching to the expected pulse train spectra. .

The findings of the work, along with a limited set of field tests on actual train-track interactions allows recommendations to be made for the deployment of sensors for cumulative damage monitoring on critical areas of track.

Dedication

To my Mother, Ranjanben Ashokkumar Thakkar

Acknowledgments

A lot of hard work and ample financial support requires finishing each and every research project. Though it is individual project, a well planned team work is essential to complete it successfully within given time period. Same happened with me so that I would like to express my strong gratitude to every individual of department of Mechanical Engineering from Heriot-Watt University - School of Engineering and Physical Science as they were directly or indirectly related to my project and I want to attribute my success to them as they truly deserve it.

First of all I want to thank heartily to my supervisors, Professor R.L. Reuben and Professor J.A. Steel, who treated through out my Ph.D. as friends and provided invaluable supervision to share their knowledge, guidance, ideas that encouraged me to perform at my best for every aspect of my research.

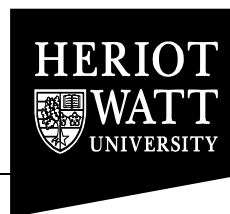
Thanks must go to my Dad (Mr. Ashokkumar N. Thakkar), my Wife (Nikita Jitendrabhai Thakkar), my family members and friends, who motivated me to complete the research with their unlimited support and love.

My special thanks go to A.I.F. Robertson, D. Dixon, R.L. Shanks, G. Knabe, K. Mackay for giving me push ups either before or during my research by working on the same project in their final year projects.

I would like to appreciate debating nature of colleague researchers Dr. P. Nivesrangsan R. Douglas, Y. Ding, N.H. Faisal, M. Shahadeh, M.S. Nashed, W. Abdou who made my subject enjoyable by providing their valuable help. I am extremely grateful to administration staff Mrs. A. Blyth, Mrs. M. Thomson, Mrs. Josie, Mrs A Campbell, Mrs. J Suttie, Mrs. I Fox, Mrs. R. Crawford and IT staff Mr. John Pritchard, Mr. Aftab Aziz, Mr. Paul Glynn for providing their daily support. At the same time I can not forget to thank technical staff of Mechanical and Electrical Engineering, Mr. A. Buchan, Mr. R. Kinsella, Mr K. Caruthers, Mr. C. Smith, Mr. A. Huston, Mr. P. Dampster and my office mates.

ACADEMIC REGISTRY

Research Thesis Submission



Name:	Nirav Ashokkumar Thakkar		
School/PGI:	School of Engineering and Physical Sciences, Mechanical Engineering		
Version: <i>(i.e. First, Resubmission, Final)</i>	Final	Degree Sought:	Ph.D.

Declaration

In accordance with the appropriate regulations I hereby submit my thesis and I declare that:

- 1) the thesis embodies the results of my own work and has been composed by myself
- 2) where appropriate, I have made acknowledgement of the work of others and have made reference to work carried out in collaboration with other persons
- 3) the thesis is the correct version of the thesis for submission*.
- 4) my thesis for the award referred to, deposited in the Heriot-Watt University Library, should be made available for loan or photocopying, subject to such conditions as the Librarian may require
- 5) I understand that as a student of the University I am required to abide by the Regulations of the University and to conform to its discipline.

* Please note that it is the responsibility of the candidate to ensure that the correct version of the thesis is submitted.

Signature of Candidate:	N.A.Thakkar	Date:	08/06/2009
-------------------------	-------------	-------	------------

Submission

Submitted By <i>(name in capitals):</i>	Nirav Ashokkumar Thakkar
Signature of Individual Submitting:	N.A.Thakkar
Date Submitted:	08/06/2009

For Completion in Academic Registry

Received in the Academic Registry by *(name in capitals):*

Method of Submission

(Handed in to Academic Registry; posted through internal/external mail):

Signature:

Date:

List of Contents

Thesis Name.....	I
Abstract.....	II
Dedication.....	III
Acknowledgements.....	IV
Table of Contents.....	VI
List of Tables.....	IX
List of Figures.....	X
Nomenclature.....	XVII
Abbreviations.....	XX
Chapter 1: Introduction.....	1
1.1 Overview.....	1
1.2 Background.....	1
1.3 Research focus.....	3
1.4 Thesis outline.....	4
1.5 Contribution to knowledge.....	5
Chapter 2: Literature Review.....	7
2.1 The mechanics of rail/wheel contact.....	7
2.2 Rail/wheel degradative processes.....	14
2.2.1 Rail/wheel wear mechanisms.....	14
2.2.2 Rolling contact fatigue (RCF).....	18
2.2.3 Wheel rolling contact fatigue (RCF).....	25
2.3 Current rail, wheel and axle monitoring techniques.....	27
2.3.1 Ultrasound-based NDT of rails and wheel sets.....	29
2.3.2 Electrical-based NDT of rails.....	34
2.4 Current remedies to increase rail life.....	35
2.5 Acoustic emission (AE) monitoring.....	40
2.5.1 AE wave propagation.....	41
2.5.2 Relevant acoustic emission (AE) applications.....	47
2.6 Summary.....	50

Chapter 3: Experimental apparatus and procedures.....	51
3.1 Experimental apparatus and test rig.....	51
3.2 Moving source (wheel) test including natural rail defects.....	55
3.3 Effect of speed and load on AE signature including flange rubbing.....	56
3.3.1 Selection of loads.....	57
3.3.2 Experimental procedure.....	57
3.3.3 Measurement of eccentricity.....	58
3.3.4 Lateral rattling elimination.....	60
3.4 Wheel defect tests.....	61
3.5 Calibration tests.....	62
3.5.1 Laboratory wave propagation test.....	62
3.5.2 Reflection and transmission tests.....	67
3.5.3 AE repeatability test.....	78
3.5.4 Wheel sleep test.....	79
3.5.5 Characterisation of natural rail defects.....	80
3.6 Summary of systematic experiments.....	82
Chapter 4: Moving source experiments.....	83
4.1 Analytical model.....	83
4.2 Establishing the time datum.....	86
4.3 Model fit to measured RMS AE.....	88
4.4 Energy calculation for different wheel speeds.....	96
4.5 Defect location.....	96
Chapter 5: Effect of speed and load on AE from rolling.....	102
5.1 Effect of speed and load on mean source energy.....	102
5.2 Wheel rattling effect.....	105
5.3 Wheel flange rubbing.....	108
5.4 Defect mapping including flange rubbing.....	112
5.5 Tests with inhibited lateral rattling.....	116
Chapter 6: Systematic wheel defect experiments.....	119
6.1 Analysis technique.....	119
6.1.1 Decomposed pulse train equation.....	121
6.1.2 Effect of two pulses.....	122
6.1.3 Simulation of wheel defects.....	126

6.2 Spatial reconstitution to remove effect of attenuation, reflection and transmission on recorded pulse-train equation.....	128
6.2.1 <i>Effect of wheel speed and load on time series</i>	129
6.3 Low frequency analysis.....	130
6.3.1 <i>Frequencies due to normal wheel rolling</i>	131
6.4 Effect of wheel defects on AE signal.....	134
Chapter 7: General discussion and conclusions.....	140
7.1 Conclusions.....	140
7.2 Future work.....	142
References.....	145

List of Tables

Table 3.1: Dimensions of the test rig.....	53
Table 3.2: Natural rail defects on track.....	81
Table 3.3: Number of test carried out through out the research.....	82
Table 4.1: Kurtosis to show correlation between AE peaks above background and mapped defects for all measurements of wheel velocities 1m/s, 1.96m/s, 3m/s, 3.5m/s and 3.84m/s.....	99
Table 6.1: Low frequency spectral peaks in moving source test.....	132
Table 6.2: Effect of impact on wheel defect wear and effect of increasing loads on wheel impact using energy per meter.....	139

List of Figures

Figure 2.1: Contact between two curved elastic bodies.....	9
Figure 2.2: Vehicle on curve ⁴⁰	11
Figure 2.3: Rolling radius difference ⁴⁰	11
Figure 2.4: Force with phase around 30° causes (a) RCF and (b) corrugation ³⁶	12
Figure 2.5: Periodic out of round of wheel ³²	17
Figure 2.6: Non-periodic out of round of wheel ³²	18
Figure 2.7: (a) Regions of white etching layer (WEL) ⁵¹ and (b) martensite layer on wheel ³⁹	18
Figure 2.8: (a) Rail rolling contact fatigue ⁵⁴ and its (b) three phases at the surface ⁵⁵	19
Figure 2.9: Isotropic hardening leading to ratchetting after RCF ⁵⁴	20
Figure 2.10: Material response to cyclic loading (a) perfectly elastic (b) elastic shakedown (c) plastic shakedown and (d) ratchetting ⁵⁵	20
Figure 2.11: Crack propagation mechanism by pressure of trapped fluid ⁴⁴	20
Figure 2.12: (a) Squat on test disc ⁴ and (b) surface shear crack generated by RCF on test Disc ⁴	22
Figure 2.13: (a) Head checks and light grey spots ³⁹ and (b) spalling ¹	23
Figure 2.14: Gauge corner cracks ⁶⁰	23
Figure 2.15: Schematic of wheel/rail contact showing shelling and detail fracture ⁶²	24
Figure 2.16: Split web crack location and orientation ⁶⁴	25
Figure 2.17: Fatigue crack growth from (a) rail head ¹ (b) bolt hole (sketch) ⁵²	25
Figure 2.18: Wheel (a) rolling contact fatigue ⁵⁴ and (b) tread shell ³⁹	26
Figure 2.19: Subsurface fatigue in railway wheels (a) shallow and (b) deep initiation ⁴⁴	27
Figure 2.20: Schematic of rail defects ⁶⁴	28
Figure 2.21: (a) Hatfield catastrophic failure ¹ (b) rail disintegration at crash site ⁶⁹	29
Figure 2.22: Principle of electromagnetic ⁸⁸	34
Figure 2.23: Corrugation analysis trolley ⁹⁸	37
Figure 2.24: Portable rail detector ⁸⁹ (a) America and (b) Europe	38
Figure 2.25: (a) Ultrasonic roller search unit (b) induction used for head	

geometries ^{89, 90}	39
Figure 2.26: High-rail ultrasonic/induction vehicle ⁸⁹ (a) American (b) European (c) Network rail test vehicle.....	39
Figure 2.27: Reflection, refraction and mode conversation of waves ¹³³ (a) Mode conversion and refraction (b) Mode conversion and reflection.....	44
Figure 2.28: Schematic diagram of zone location method (a) using the highest amplitude and (b) using the highest and second highest signal amplitude ¹³⁵	46
Figure 3.1: Test Rig (a) layout for rolling trials (b) schematic diagram showing sensor array for propagation tests (c) detail of bearing housing, shaft and wheel assembly on rail.....	52
Figure 3.2: (a) Motor 1 (b) Motor 2 mounted underneath table and (c) fish plate joint.....	53
Figure 3.3: 4-Channel data acquisition system with connector block, signal conditioning unit, preamplifier, and vacuum grease.....	54
Figure 3.4: (a) Hsu-Nielsen source and (b) guide ring ¹³³	55
Figure 3.5: Experimental set-ups used for moving source test.....	56
Figure 3.6: Experimental set-up for load test (a) sensor positions on rail with applied external load (b) dead loads on supporting arm.....	57
Figure 3.7: (a) Motor shaft displacement and (b) dial gauge mounted on supporting arm.....	59
Figure 3.8 Measured points and fitted and nominal circles (a) to scale and (b) with amplified radial scale.....	59
Figure 3.9: Reduction in shaft play from (a) 1.55mm to (b) 0.55mm.....	60
Figure 3.10: Schematic of simulated defects (flats) around the circumference of wheel...	61
Figure 3.11: Schematic diagram of sensor positions for propagation tests. ‘T’ signifies trigger sensor.....	63
Figure 3.12: Absolute AE signals recorded at 3 arrays of 4 sensors.....	64
Figure 3.13: Magnified wave arrival at S ₄ of array 3 from figure 3.12.....	65
Figure 3.14: (a) Example of apparent velocity of fast wave but with poor correlation (b) effect of threshold on apparent velocity.....	66
Figure 3.15: Velocities of (a) fast wave with threshold set at 0.025 V and (b) slow wave with threshold set at 0.16.....	66
Figure 3.16: Attenuation coefficients for (a) fast wave and (b) slow wave.....	67

Figure 3.17: Sensor arrays for reflection/transmission tests in which the second sensor distance increased from the joint (a) array 1 and (b) array 2.....	68
Figure 3.18: Absolute values of raw AE signals when sensor 2 is (a) 0.26m and (b) 0.52m away from joint.....	69
Figure 3.19: Measured absolute raw AE at sensors (a) 2 and (b) 3, with sensors positioned 0.26mm from the joint.....	69
Figure 3.20: Measured absolute raw AE at sensors 2, positioned 0.52mm from the joint...70	70
Figure 3.21: Schematic diagram for determination of reflection coefficient, from records at sensor 2 for array 1 and array 2 (a) Array 1, sensor 2 0.26m from joint and (b) Array 2, sensor 0.52m from joint.....	76
Figure 3.22: Schematic diagram for determination of transmission coefficient, from records at sensor 2 and sensor 3 of array (a) Array 1, sensor 3 (105mm from source) and (b) Array 1, sensor 3 (440mm from source).....	77
Figure 3.23: Sensor positions for AE reliability test.....	78
Figure 3.24: Testing of repeatability of energy using H-N source.....	79
Figure 3.25: Scaled wheel and rail used for slip test.....	79
Figure 3.26: Outline of how wheel divisions match track divisions during motion.....	80
Figure 3.27: High speed camera result for a wheel speed of 3.5m/s and 4 kg-6.5 kg external load (a) Wheel distance travel against time and (b) Wheel rotation angle against time.....	80
Figure 4.1: Definition of distances for wheel position between joint (J) and sensor (S)...84	84
Figure 4.2: Definition of distances for wheel position between sensor (S) and joint (J)...85	85
Figure 4.3: (a) Full AE record and (b) magnified record close to trigger for each of the wheel speeds.....	88
Figure 4.4: Measured RMS AE at sensor S, wheel speed 3.5m/s. _____ RMS AE; _____ analytical model.....	90
Figure 4.5: Measured RMS AE at sensor S, wheel speed (a) 1m/s and (b) 1.96m/s. _____ RMS AE; _____ analytical model.....	91
Figure 4.6: Measured RMS AE at sensor S, wheel speed (a) 3m/s and (b) 3.84m/s. _____ RMS AE; _____ analytical model.....	92
Figure 4.7: Source AE energy as function of distance for wheel speed 1m/s.....	93
Figure 4.8: Source AE energy as function of distance for wheel speed 3.5m/s.....	93
Figure 4.9: Mean source energy E_0 (V^2s) as a function of track speed, for wheel moving	

away from sensor (closed) and wheel approaching sensor (open).....	94
Figure 4.10: Measured RMS AE at sensor S, wheel speed 3.5m/s. _____RMS AE; ——analytical model using normalized averaged E_0 value for whole circumference.....	95
Figure 4.11: Mean source energy E_0 (V^2s) as a function of track speed using normalized averaged E_0 value for whole circumference.....	95
Figure 4.12: Energy in absolute signal for increasing wheel speeds (a) in entire record after pre-trigger and (b) in one wheel rotation when wheel is above sensor.....	96
Figure 4.13: Lap defect on running surface of rail between distances of 0.39 and 0.43 m from the joint (i.e. defect length approximately 5cm).....	97
Figure 4.14: Measured RMS AE (dotted curve) in 0.1m steps above normal rolling and summation of mapped defects in 0.1m distance (solid curve) at various wheel speeds (a) Velocity of wheel 1 m/s (b) Velocity of wheel 1.96 m/s (c) Velocity of wheel 3 m/s (d) Velocity of wheel 3.5 m/s.....	97
Figure 4.15: Cross correlation of Measured RMS AE (0.1m steps) above normal rolling and summation of mapped defects in 0.1m distance for a uniform source at various wheel speeds (a) Velocity of wheel 1 m/s (b) Velocity of wheel 1.96 m/s (c) Velocity of wheel 3 m/s (d) Velocity of wheel 3.5 m/s.....	98
Figure 4.16: Measured RMS AE (dotted curve) in 0.1m steps above normal rolling and summation of mapped defects in 0.1m distance (solid curve) at various wheel speeds for normalized average E_0 value.....	100
Figure 4.17: Cross correlation of Measured RMS AE (0.1m steps) above normal rolling and summation of mapped defects in 0.1m distance for a uniform source at wheel speeds using normalized average E_0 value.....	101
Figure 5.1: Mean source energy E_0 (V^2s) as a function of track speed and 4kg load, for wheel moving away from sensor (solid) and wheel approaching sensor (hollow).....	103
Figure 5.2: Mean source energy E_0 (V^2s) as a function of track speed and 5kg load, for wheel moving away from sensor (solid) and wheel approaching sensor (hollow).....	103
Figure 5.3: Mean source energy E_0 (V^2s) as a function of track speed and 6kg load, for wheel moving away from sensor (solid) and wheel approaching sensor (hollow).....	104
Figure 5.4: Mean source energy E_0 (V^2s) as a function of track speed and 6.5kg load, for wheel moving away from sensor (solid) and wheel approaching sensor (hollow).....	104
Figure 5.5: Rattling effect on RMS signal.....	105
Figure 5.6: Energy per wheel rotation for increasing wheel speed (a) 4kg load	

(b) 5kg load (c) 6kg load (d) 6.5kg load.....	106
Figure 5.7: Energy per wheel rotation for increasing wheel speed (extended test) (a) 4kg load (b) 4.5kg load.....	107
Figure 5.8: (Load test) Energy calculation per wheel rotation.....	107
Figure 5.9: Natural defects between 1.46 m and 1.58m clockwise from joint.....	108
Figure 5.10: Measured RMS AE (light solid line) and analytical model (dark solid line) at 4kg load and wheel speed (a) 1m/s and (b) 1.96m/s.....	109
Figure 5.11: Measured RMS AE (light solid line) and analytical model (dark solid line) for lower speeds and all loads.....	110
Figure 5.12: Measured RMS AE (light solid line) and analytical model (dark solid line) for higher speeds and all loads.....	111
Figure 5.13: Energy calculated for the 0.56m wheel flange rubbing arc for increasing wheel speed (a) 4kg load (b) 5kg load (c) 6kg load and (d) 6.5kg load.....	112
Figure 5.14: Signal above normal rolling and defect intensity without flange rubbing for wheel speed 3.5m/s and 4kg load condition.....	113
Figure 5.15: Cross correlation between defect intensity and AE above normal rolling without flange rubbing for wheel speed 3.5m/s and 4kg load condition.....	113
Figure 5.16: Signal above normal rolling and defect intensity with flange rubbing for wheel speed 3.5m/s and 4kg load condition.....	114
Figure 5.17: Cross correlation between defect intensity and AE above normal rolling with flange rubbing for wheel speed 3.5m/s and 4kg load condition.....	114
Figure 5.18: Kurtosis with and without flange rubbing for all wheel speeds and at 4kg load. (Conditions 1-4, 1ms^{-1} , 1.5ms^{-1} , 3ms^{-1} and 3.5ms^{-1} , respectively).....	115
Figure 5.19: Average kurtosis of cross-correlation between defects and AE above rolling background, with and without consideration of flange rubbing (Speed conditions 1-4, $1=1\text{ms}^{-1}$, $2=1.5\text{ms}^{-1}$, $3=3\text{ms}^{-1}$, $4=3.5\text{ms}^{-1}$, respectively).....	116
Figure 5.20: Energy calculated for the 0.56 m distance during flange rubbing plotted against wheel speed (1mm spacer test).....	117
Figure 5.21: Energy calculated for the 0.56 m distance during flange rubbing plotted against axle load (1mm spacer test).....	117
Figure 5.22: Energy per wheel rotation 0.05m after joint plotted against wheel speed (1mm spacer test).....	118

Figure 5.23: Energy per wheel rotation 0.05m after joint plotted against axle load (1mm spacer test).....	118
Figure 6.1: Calculated spectrum of a square wave, showing effect of increase in amplitude (a) $A = 1$ and (b) $A = 2$	120
Figure 6.2: Calculated frequency domain of pulse train ($k_1=0.2, T_c=1, d_1=0.2, 1/d_1=5$), effect of increase in amplitude (a) $A = 1$ and (b) $A = 2$	120
Figure 6.3: Calculated frequency domain of pulse train ($A=1, T_c=1$), effect of pulse width (a) $k_1=0.2, 1/d_1=5$ (b) $k_1=0.1, 1/d_1=10$	121
Figure 6.4: Calculated frequency domain of pulse train ($k_1=0.2, A=1$), effect of period. (a) $T_c=1, 1/d_1=5$ (b) $T_c=2, 1/d_1=10$	121
Figure 6.5: Constants ($A=0.5, C=0, k_c=0.1, T_c=1, d=0.1, 1/d=10, \phi_1=\pi$), variable ($B=0.5$) (a) Time domain (b) Calculated frequency domain of pulse train.....	123
Figure 6.6: Constants ($A=0.5, C=0, k_c=0.1, T_c=1, d=0.1, 1/d=10, \phi_1=\pi$), variable ($B=0.25$) Time domain (b) Calculated frequency domain of pulse train.....	123
Figure 6.7: Constants ($A=0.5, C=0, k_c=0.1, T_c=1, d=0.1, 1/d=10, \phi_1=\pi$), variable ($B=0.125$) (a) Time domain (b) Calculated frequency domain of pulse train.....	123
Figure 6.8: Constants ($A=0.5, C=0, k_c=0.1, T_c=1, d=0.1, 1/d=10, \phi_1=\pi$), variable ($B=0$) (a) Time domain (b) Calculated frequency domain of pulse train.....	124
Figure 6.9: Constants ($A=0.5, B=0.5, C=0, k_c=0.1, T_c=1, d=0.1$), variable ($\phi_1=\pi$) (a) Time domain (b) Calculated frequency domain of pulse train.....	124
Figure 6.10: Constants ($A=0.5, B=0.5, C=0, k_c=0.1, T_c=1, d=0.1$), variable ($\phi_1=\pi/2$) (a) Time domain (b) Calculated frequency domain of pulse train.....	125
Figure 6.11: Constants ($A=0.5, B=0.5, C=0, k_c=0.1, T_c=1, d=0.1$), variable ($\phi_1=\pi/3$) (a) Time domain (b) Calculated frequency domain of pulse train.....	125
Figure 6.12: Constants ($A=0.5, B=0.5, C=0, k_c=0.1, T_c=1, d=0.1$), variable ($\phi_1=\pi/4$) (a) Time domain (b) Calculated frequency domain of pulse train.....	125
Figure 6.13: Simulated pulses with phase difference as in wheel flat test, pulse height proportional to chord width and pulse widths are $k_1=0.3, k_2=0.2$ and $k_3=0.1$	126
Figure 6.14: Calculated frequency domain of pulse train with different amplitudes, widths and phase differences (a) Magnified (b) Highly magnified.....	127
Figure 6.15: FFT using periodogram of simulated pulse train with fixed amplitude ratios,	

and phase differences, with variable width.....	127
Figure 6.16: Original (a) and reconstituted (b) RMS AE record for wheel velocity 1m/s and 6kg load.....	128
Figure 6.17: Typical reconstituted RMS AE records; (a) 1m/s and 4kg; (b) 1m/s and 6kg; (d) 3m/s and 4kg; (e) 3m/s and 6kg. Figure (c) shows magnified part of Figure (a).....	129
Figure 6.18: FFTs of reconstituted signals shown in Figure 6.17 (a), (b), (d) and (e).....	131
Figure 6.19: Reconstituted moving source test record at 1m/s and 4kg, (a) normalised spectra (b) magnified spectra (c) averaged spectrum and (d) magnification of (c)...	132
Figure 6.20: Time, distance and frequency domains for long time-records, 1.5m/s and 4kg (a) Time domain (RMS) (b) Distance domain (RMS) (c) Spectrum (d) Magnified Spectrum.....	134
Figure 6.21: Spectra for longer recording time at 1.5m/s (a) 5kg (b) Magnified, 5kg (c) 6kg (d) Magnified, 6kg (d) 6.5kg (e) Magnified, 6.5kg.....	135
Figure 6.22: Spectra for longer recording time at 4 kg load (a) 2m/s (b) Magnification of (a) (c) 3m/s (d) Magnification of (c)(e) 3.5m/s (f) Magnification of (e).....	137
Figure 6.23: FFTs of reconstituted signals shown in Figure 6.17 (d) and (e) with high pass filter to remove track rotational frequency.....	137
Figure 6.24: Reconstituted time domain signals for the five wheel defect runs under conditions (a) 1m/s and 4kg (b) 1m/s and 6kg (c) 3m/s and 4kg (d) 3m/s and 6kg (x-axis is time (sec) and y-axis is amplitude (arbitrary units)).....	138
Figure 6.25: Reconstituted frequency domain signals for the five wheel defect runs under conditions (a) 1m/s and 4kg (b) 1m/s and 6kg (c) 3m/s and 4kg (d) 3m/s and 6kg (x-axis is frequency (Hz) and y-axis is power (arbitrary units)).....	139
Figure 7.1: Smoothed RMS AE compared with model.....	144

Nomenclature

a, b	Semi-axes of the contact ellipse
a_0	Crack depth (m)
A	Amplitude of the 1 st pulse (V)
A_0	Amplitude at source (V)
A_1	Amplitude at distance x from the source (V)
A_w	Wave amplitude (V)
da_0/dN	Crack growth rate (m/cycle)
β_1	Angle of refraction ($^\circ$)
B	Amplitude of the 2 nd pulse (V)
B_1	Magnetic field (Teslas)
c	Wave velocity (m/s)
c_1	Track circumference (m)
c_2	Distance between the joint and sensor (m)
C	Amplitude of the 3 rd pulse (V)
C_{HF}	High frequency wave velocity (m/s)
C_{LF}	Low frequency wave velocity (m/s)
d_1	Distance from source to first sensor (m)
D	Distance between the two sensors (m)
D_1	Source to sensor distance (m)
D_r	Rolling distance (m)
E	Young's modulus
E_0	Energy of the source (V^2s)
E_1	Young's modulus of 1 st elastic body
E_2	Young's modulus of 2 nd elastic body
E_g	Acoustic emission energy (V^2s)
E_x	AE energy at distance x from the source (V^2s)
E_{1x}	AE energy of sensor 1 at distance x from the source (V^2s)
E_{2x}	AE energy of sensor 2 at distance x from the source (V^2s)
E_{3x}	AE energy of sensor 3 at distance x from the source (V^2s)
E_r	Energy associated with rolling (Nm)

E_t	Energy at time, t , when the moving source is x distance from sensor (V^2s)
E_{t1}	Total AE energy recorded at the sensor over the time step (V^2s)
E_T	Energy from the fixed time window, T_w , of 0.17ms (V^2s)
f	Frequency (Hz)
F_L	Lorentz force (N)
J_e	Eddy current (Amperes)
J	Joint
k	Attenuation coefficient (m^{-1})
k_1, k_2, k_3, k_c	Pulse widths
ΔK	Stress intensity exposure ($MNm^{-3/2}$)
L	Normal load (N)
m	Constant
n	Constant
n_1	Index of refraction of incident medium
n_2	Index of refraction of refraction medium
nw	Number of wheels
N	Number of fatigue cycles
N_1	Normal load (N)
p_0	Maximum contact pressure (N)
r	Distance (m)
R_c	Radius of curvature (m)
R	Reflection coefficient
R_e	Radius of track (m)
R_{c1}	Radius of curvature of 1 st elastic body (m)
R_{c2}	Radius of curvature of 2 nd elastic body (m)
R^2	Correlation factor
S, S_1, S_2, S_3, S_4	Sensors positions
t	Time (s)
Δt	Arrival time difference between two sensors (s)
Δt_1	Arrival time difference between wave modes (s)
T_w	Time window (s)
T	Transmission coefficient
T_c	Cycle time or period (s)

T_m	Magnitude of creep force (N)
$v(t)$	Amplitude of the AE waveform (V)
x, x_1	Source sensor distance (m)
x_{mw}	Source sensor distances (different for each wheel)
X	Longitudinal component of creep force (N)
Y	Lateral component of creep force (N)
$z_0(x,y)$	Initial contact between two curved bodies
Z_1	Acoustic impedance of Medium 1 ($\text{kg/m}^2\text{s}$)
Z_2	Acoustic impedance of Medium 2 ($\text{kg/m}^2\text{s}$)
μ	Friction coefficient
Ω_{slip}	Slip region
Ω_{stick}	Stick region
$s(x, y)$	Relative slip velocity (m/s)
$\tau(x,y)$	Tangential stress (N/m^2)
θ	Phase of creep force ($^\circ$)
θ_1	Angle of incidence ($^\circ$)
ϕ_1	Phase angle between 1 st and 2 nd pulse
ϕ_2	Phase angle between 1 st and 3 rd pulse

Abbreviations

AE	Acoustic emission
ALE	Adaptive line enhancer
ASTM	American society of testing materials
BCF	Bearing characteristic frequency
DAQ	Data acquisition
DFR	Demodulated frequency resonance
EDM	Electro discharge machining
EM	Electromagnetic
ES	Electrostatic
EMATs	Electro magnetic acoustic transducers
FEA	Finite element analysis
FFT	Fast Fourier transform
GCC	Gauge corner cracking
HCT	Hertz's contact theory
HSDI	High speed diesel
MGT	Mean gross tonnage
NDE	Non destructive evaluation
NDT	Non destructive testing
NI	National instruments
NOWL	No white layer
OOR	Out of round
PRD	Portable rail detector
PSD	Power spectral density
PZT	Lead zirconate titanate
RCM	Reliability centred maintenance
RCF	Rolling contact fatigue
RMS	Root mean square
rpm	Revolution per minute
RSU	Roller search unit
SEM	Scanning electron microscope

WEL

White etching layer

WL

White layer